Supplementary Materials: XRD on Clover Creek Samples.

Dagmar Dietrich and Thomas Mehner

1. Introduction

Schuster [1] described the wood as turned to opal, given that the majority of the petrifying material is opal with the opal in the vessels showing signs of change by formation of spherulitic chalcedony. Moreover, the devitrification in the vessels did not originate in the tyloses. Additionally, he suspected from his observations monoclinic calcium oxalate crystals in parts of the large medullary rays and hydrated ferric oxide in darker sections of the sample.

Mitchel and Tuft [2] studied a variety of opalized fossil wood from Australia, Hungary, Japan and Northern America including samples from "Idaho/Lincoln County" and "Idaho/Clover Creek (?)". The major phase in most of the samples including samples from Idaho was indicated as disordered tridymite, either alone or with quartz (rarely the presence of one or more additional weak X-ray reflections suggesting calcite, cristobalite, or unknown substances).

Opal exists in a number of structural states that are designated opal-A, opal-CT, and opal-C, where A, C, and T signify amorphous, cristobalite, and tridymite, respectively (Jones and Segnit [3]). Opal-CT has long been recognized as being structurally similar to cristobalite and tridymite. Early inferences were based on a qualitative interpretation of X-ray diffraction (XRD) patterns. At least as early as 1955 (Flörke, 1955, in Jones and Segnit [3]), it was recognized that diffraction patterns are consistent with cristobalite that contains stacking disorder, i.e., interstratified cristobalite and tridymite. Guthrie et al. [4] simulated XRD patterns for opal-CT and compared them to several natural opal-CT specimens. Stacking of idealized sheets of the high-temperature structures of cristobalite and tridymite were used for the calculations. Modeling opal-CT as interstratified layers of cristobalite and tridymite reproduced the dominant features of the opal-CT XRD patterns (shapes, positions, and widths of the 19.5°–24.5° 2θ band and the 35.9° 2θ peak). The range for the opal crystallite sizes, around 15 nm, is in excellent agreement with the crystallite sizes determined on different opal-CT samples using TEM published by Elzea and Rice [5]. Furthermore, the increasing opal-CT maturity which is typically monitored by the position of the 21.7° 2θ peak is reflected by the simulations of Guthrie et al. [4] and is in accordance with the increasing crystallite size. Mostly reported as "d_{101} peak" of the tetragonal phase (and equivalent to the "d_{111} peak" of cubic cristobalite), the peak migrates from 0.412 to 0.404 nm during diagenesis. Recently, combined XRD and Raman spectroscopic investigations on volcanic opals by Ostrooumov [6] evidenced that the shift towards higher d-spacing can be explained by the unresolved superposition of cristobalite and tridymite reflections in the pattern due to the increasing amount of tridymite stacking.

Elzea and Rice [5] succeeded to confirm by TEM studies crystallite sizes in opal-CT as well as that the opal polymorphs represent a continuous series of disordered intergrowths between the end-members cristobalite and tridymite in the stacking sequences. By using mean crystallite sizes directly measured from TEM images, XRD line broadening due to crystallite size could be distinguished from that due to structural disorder by Guthrie *et al.* [4].

2. Experimental Method

The sample was sliced by means of a diamond cutting wheel, cleaned by pure ethanol and air-dried. For powder diffraction a part of the sample was covered in a plastic-bag and crashed by a hammer (thus avoiding the use of an agate mortar and pestle). X-Ray Diffraction (XRD) analysis by means of a diffractometer D8 Discover (Bruker AXS, Karlsruhe, Germany) was applied for the determination of the phases under consideration of local differences in phase ratios, crystallite sizes and microstrains. The diffractometer is equipped with an X-ray tube with a Cu anode (40 kV, 40 mA), a Ni filter for monochromatization, polycap optics, a 0.5 mm collimator and a point detector (SOL-XE) with a 0.6 mm detector slit. The sample was scanned from 15° to 85° 2θ with a 0.02° 2θ step size

and 16 s per step data collection time. Line widths were evaluated by means of the program TOPAS under consideration of the device-related line-broadening effects to estimate the coherence length.

3. Results

Figure S1 shows the diffraction diagrams of the sliced sample at a position containing a significant portion of quartz and the powdered sample. The mineral phases α-quartz, monoclinic low-tridymite and cubic high-cristobalite are indicated. Different fit variants were applied to the data comprising an amorphous cristobalite phase, the low-temperature tetragonal phase of cristobalite and monoclinic tridymite with different superstructures and intermediate phases, which all can coexist in opal-CT. A fit using trigonal α-quartz (PDF 01-075-8322, a = 0.4917 nm, c = 0.5410 nm), cubic cristobalite (PDF 01-085-0621, a = 0.711998 nm) and monoclinic tridymite (PDF 01-074-8988, a = 2.5878 nm, b = 0.5001 nm, c = 1.8526 nm) was favored where the quartz fraction in general does not exceed 40%, the cristobalite/tridymite ratio varies only slightly with the size of the crystallites (in the sense of coherently scattering domains) being almost similar for both phases. Additionally, the ~21.7° 2θ peak position (indicated according to the cristobalite phase as d_{110} or d_{111}) evidenced almost fixed for sample parts with the high opal/low quartz content. Additionally, the microstrains in all phases are lowest.

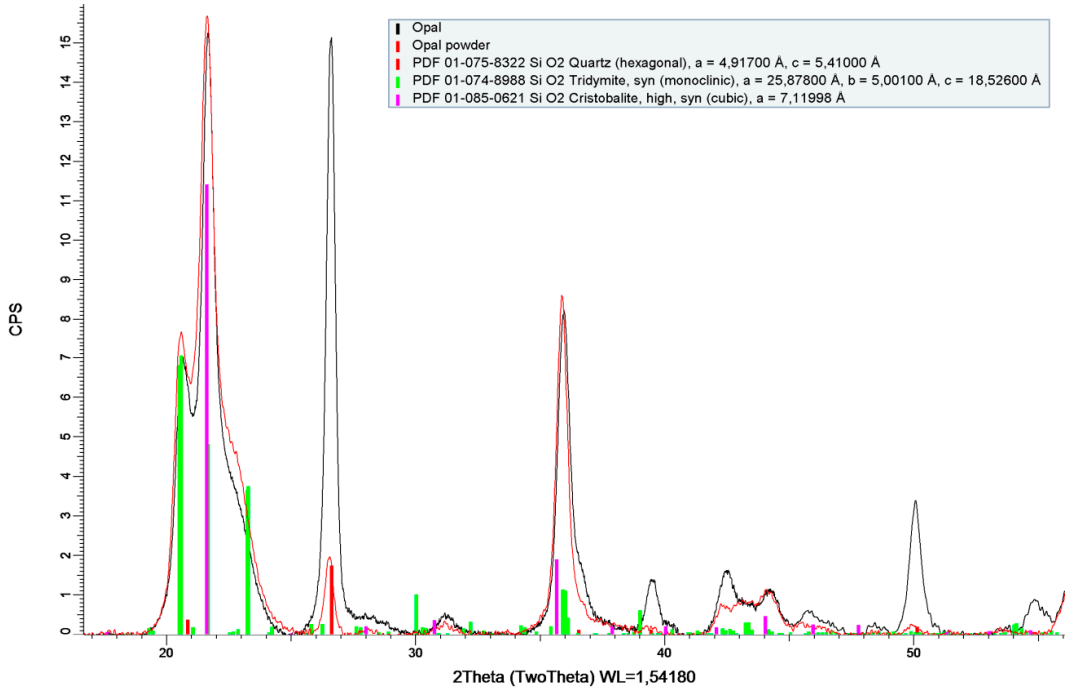

Figure S1. Diffraction diagrams of the opalized wood (red—powder, black—example for a distict position on the cross-section).

We refer to the publication of Puhlmann and Bohrmann [7] that evidenced cristobalite clusters with cubic structure in opal at room temperature. Hatch and Ghose [8] discussed the α-β cristobalite transition as a fluctuation-induced first-order transition. Zhang and Scott [9] confirmed the β-phase as a dynamic average of α-type domains. Accordingly, the α-β cristobalite transition can be perceived as fluctuation induced. The α-cristobalite structure is than a dynamic average in space and time of cubic β-cristobalite type domains. The transformation proceeds by flipping between twin related low temperature domains which begins well below and continues above the transition temperature.

The complexity of the cristobalite and tridymite structures is substantiated by the diffusion model for silica transport and accumulation in sedimentary environments established by Landmesser [10]. His concept of ''mobility by metastability'' is based on the presence of various metastable forms of silica and a sluggish ripening process from amorphous silica via opal and chalcedony to quartz. The heterogeneity of silica is therefore considered as a result of the extreme sluggishness of the silica

phase transformation processes at ambient temperatures.

Phase fractions, crystallite sizes and lattice spacing according to preferred fit are summarized in Table S1. The mineral content of the Cover Creek sample is mostly opal-CT with a cristobalite/tridymite ratio around 0.54 and crystallite sizes around 22 nm. Opal-CT/ α-quartz fractions depend on the position of the X-ray beam at the sample and changes with respect to the former wood structure. Remarkable α-quartz content is evidenced in the area of the large vessels of the early-wood.

Table S1. Phase fractions, crystallite sizes and lattice spacing according to the ~21.7° 2θ peak position for different sample positions and the sample powder (d_{101} according to a fit using low-cristobalite).

Position	Phase	Fraction	Size (nm)	d_{111} (nm)	d_{101} (nm)
1	cristobalite	0.31	31 ± 4	0.4088	0.4083
	tridymite	0.64	21 ± 2	--	
	α-quartz	0.05	58 ± 7	--	--
2	cristobalite	0.26	22 ± 1	0.4092	0.4076
	tridymite	0.71	25 ± 2	--	
	α-quartz	0.03	81 ± 17	--	--
3	cristobalite	0.48	22 ± 2	0.4078	0.4077
	tridymite	0.22	16 ± 1	--	
	α-quartz	0.30	55 ± 2	--	--
4	cristobalite	0.34	16 ± 1	0.4086	0.4081
	tridymite	0.64	27 ± 2	--	
	α-quartz	0.02	68 ± 23	--	--
5	cristobalite	0.35	17 ± 1	0.4089	0.4081
	tridymite	0.64	26 ± 2	--	
	α-quartz	0.01	>300	--	--
Powder	cristobalite	0.35	15 ± 1	0.4096	0.4093
	tridymite	0.61	25 ± 2	--	
	α-quartz	0.04	55 ± 12	--	--

The crystal size in the phase α-quartz is generally low (between 60 and 80 nm, occasionally >300 nm). This is consistent with the expectation that cryptocrystalline modifications of fibrous chalcedony or granular jasper occur in silicified wood. These modifications are composed of fine intergrowths of alpha-quartz and moganite. The remarkably small crystallite size of α-quartz matches well the relatively high amount of moganite found by RAMAN spectroscopy. Moganite was not detected by XRD; probably because Moganite occurs in chalcedony as nano-range lamellae down to single Brazil law twin planes which are too small for the long-range order dependent XRD.

The opal-CT crystal sizes are on average (20 ± 5) nm for cristobalite and tridymite, both. According to the current approach to monitoring opal maturation using the 21.7° 2θ peak position (typically reported as cristobalite d_{101}), we receive a lattice spacing d_{111} = 0.409 nm. The indexing is coherent with the cubic phase of cristobalite; interestingly, using triclinic low-temperature cristobalite for the fit results in a corresponding lattice spacing d_{101} = 0.408 nm.

References

1. Schuster, J. Über ein pliocänes Eichenholz aus Idaho. *Neue Jahrb. Mineral. Geol. Pal.* **1908**, *2*, 49–54.
2. Mitchel, R.S.; Tuft, S. Wood Opal - A Tridymite-like Mineral. *Am. Mineral.* **1973**, *58*, 717–720.
3. Jones, J.B.; Segnit, E.R. The nature of opal. I. Nomenclature and constituent phases. *J. Geol. Soc. Australia* **1971,** *18*, 57–68.
4. Guthrie JR., G.D.; Dish, D.L.; Reynolds JR., R.C. Modeling the X-ray diffraction pattern of opal-CT. *Am. Mineral.* **1995**, *80*, 869–872.
5. Elzea, J.M.; Rice, S.B. TEM and X-ray diffraction evidence for cristobalite and tridymite stacking sequences in opal. *Clay. Clay Miner.* **1996**, *44*, 492–500.
6. Ostrooumov, M. A Raman, infrared and XRD analysis of the instability in volcanic opals from Mexico. *Spectrochim. Acta A* **2007**, *68*, 1070–1076.
7. Puhlmann, P.W.; Bohrmann, G. Partiellkristalline Strukturbildungen im System Opal-CT. Ein Neuansatz. 2000, http://www.chemie.uni-jena.de/DGK-AK4/VOR_00/pwp.pdf (accessed on 17 February 2015).
8. Hatch, D.M.; Ghose, S. The α-β Phase Transition in Cristobalite, SiO2 - Symmetry Analysis, Domain Structure, and the Dynamical Nature of the β-phase. *Phys. Chem. Miner.* **1991**, *17*, 554–562.
9. Zhang, M.; Scott, J.F. Raman studies of oxide minerals: a retrospective on cristobalite phases. *J. Phys. Condens. Matter* **2007**, *19*, doi:10.1088/0953-8984/19/27/275201.
10. Landmesser M. Mobilität durch Metastabilität: SiO2 Transport und Akkumulation bei niedrigen Temperaturen. *Chem. Erde* **1995**, *55*,149–176.